



## Optimization of Surface Plasmon Resonance (SPR) for Gold/Air Interface by using Kretschmann Configuration

Yadgar H. Shwan\* , Berun N. Ghafoor  , Govar H. Hamasalih

Physics Dept., University of Sulaimani, Sulaimani 46001, Iraq.

\*Corresponding author Email: <mailto:yadgar.shwan@univsul.edu.iq>

### HIGHLIGHTS

- The greatest SPR achieved in angle of  $45.1^\circ$  at  $50\text{nm}$  of gold.
- The perfect region of SPR for the gold layer was in the range  $(40 - 50)\text{nm}$ .
- SPR for gold/air depends on incident angle, refractive index, or dielectric medium and thickness.

### ABSTRACT

The coherent oscillation of electrons at contact among a dielectric and metal when the metal is exposed to incoming plasmon is known as “surface Plasmon resonance”. To achieve the best surface plasmon resonance (SPR) signal, several aspects must be considered, including the excitation wavelength, the sort of metals used, and the thickness of the metal layer. The modification of the surface plasmon resonance (SPR) depending on the thickness of metallic gold was investigated in this study. The reflection spectrum is determined as a function of metal thickness and dielectric medium (air), which is fixed in this case, and measuring the resonance angle for each size (length of the gold layer) to visualize the influence of the metal film on the resonance angle. The analysis concentrated on the impact of gold layer thickness variations on resonance angle shift. SPR's ideal thickness was discovered to be 45-50 nm. We used the spin coating method to create a thin layer. The thickness of thin films is measured by scanning the sample with an atomic force microscope (AFM) tip. The optimum SPR angle profile with the minimum amount of reflection and dip reflection is achieved with this film thickness. The reflectance and resonance angle performance features of gold layers were analyzed utilizing plasmonic Kretschmann configurations at a wavelength (632.8 nm) in sensing media (air). In an experimental analysis of the improved surface plasmon resonance characteristics of the gold/air coupling, they also showed a significant shift in resonance angle due to the film thickness variation. Biomedical science, optics, biosensing, and medicine are just a few of the domains where the (SPR) has been applied.

### ARTICLE INFO

**Handling editor: Akram R. Jabur**

#### Keywords:

SPR  
Resonance Angle  
Reflection  
Gold layer  
Plasmon waves

## 1. Introduction

A charge-density resonance that propagates along the surface of a metal-dielectric medium is known as a surface plasmon. Once the dielectric-metal interface strikes with a polarized beam under the condition of total internal reflection, the electrons on metal are excited about a resonance frequency, referred to as surface plasmon waves generated *SPW*, wave of the resonance known as the evanescent wave. The qualities of the gold layer, such as dielectric, have an impact on the surface wave, and that can react with an external medium, which is why it could be utilized as a biosensor. One of the methods in this excitation is the Kretschmann configuration, as illustrated in Figure 1 [1]. The (beam's wave and plasmon's wave) vector is equivalent at a given angle of incidence. This is coming from a study of how the (*angle resonance*) varies as the (*angle incidence*) whereas its wavelength remains unchanged ( $\lambda = 632.8\text{ nm}$ ). A dip pattern in the curve and minimal reflection  $R_{min}$  are two more characteristics of this spectrum, and the FWHM (full width half maximum) has been conducted for each peak of the reflectance spectrum. The minimal reflection  $R_{min}$  refers to the vast amount of light energy converted to electrons metal, resulting in the smallest amount of light returned to the detector, known as R min, and the resonance is generated in this situation. The precious metals Au are more typically utilized to spread (SPW) at a visible range [2- 4]. We'll show which thickness of gold is great for producing SPR, as well as which angle provides the best SPR by constant refractive index.

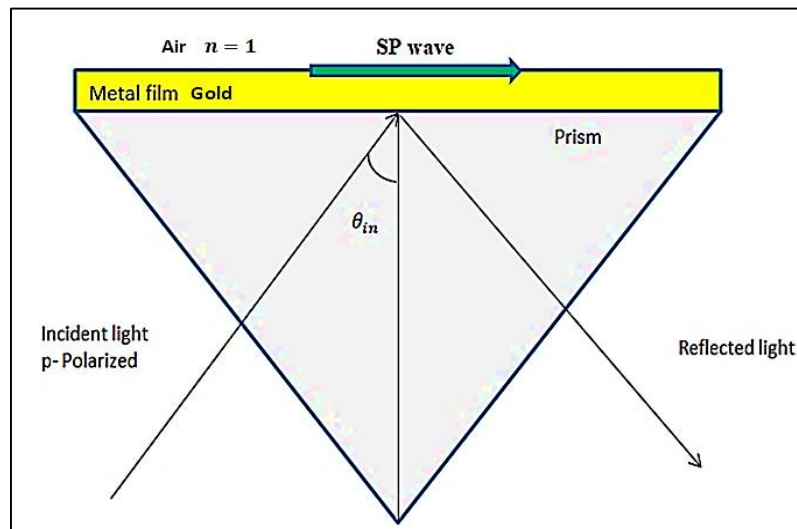


Figure 1: Kretschmann configuration of the SPW on gold/air interface

The metal layer (film thickness) designated has a massive effect on the SPR sensor's performance. Metals such as gold are preferred so that they can resonate electrons at an appropriate frequency. In most situations, gold has been used as a metal layer since it is chemically stable, has low oxidation, and is immune to air pollutants. It has a higher detection accuracy at visible wavelength relative to other metals. SPR becomes a more common occurrence as that was discovered that label-free detection techniques are appropriate and dependable for clinical analysis and biomolecular interactions. The SPR device's performance (sensitivity) is determined by metal layer optimization [5-9]. It has been observed that a material has the lowest amount of reflection at a given angle (resonance angle) compared to the other angle [10]. Equation (1) would be used to determine reflectance as a function of incident angle for dual interface (metal-dielectric), which differs from refractive index and dielectric displays in Figure 2.

$$r_p = \frac{\left[ n_1 \sqrt{1 - \left( \frac{n_1}{n_2} \cos \theta_{in} \right)^2} - n_2 \cos \theta_{in} \right]^2}{\left[ n_1 \sqrt{1 - \left( \frac{n_1}{n_2} \cos \theta_{in} \right)^2} + n_2 \cos \theta_{in} \right]^2} \tag{1}$$

$r_p$ : Reflection for p-polarization light,  $n_1$  and  $n_2$  are the refractive index of the first and second medium,  $\theta_{in}$ : Incident angle of the laser beam.

In a total reflection setup, mono light p-polarized impacts directly on a prism and interacts with gold. Evanescent waves are created when light interacts with a gold coating, leading electrons to accumulate on the surface. Once the SPW is released at the gold/air boundary with a fixed angle, the intensity would drop to the lowest when the plasmon wave is coupled [11]. The Kretschmann configuration is one of several ways that have been utilized to combine evanescent waves into surface plasmon waves (SPW). When an extremely thin film is placed at the interface between two media, free electrons in the metal sheet could interact with incoming light within a restricted range (SPR angle). As a result, a charge density beam passes over a metal sheet, and the amplitude of charge density is located in the second medium, which is totally different from the dielectric. This situation is referred to as (resonance plasmon). This surface plasmon is resonantly excited by the incoming light's evanescent wave, as illustrated in Figure 3 [12].

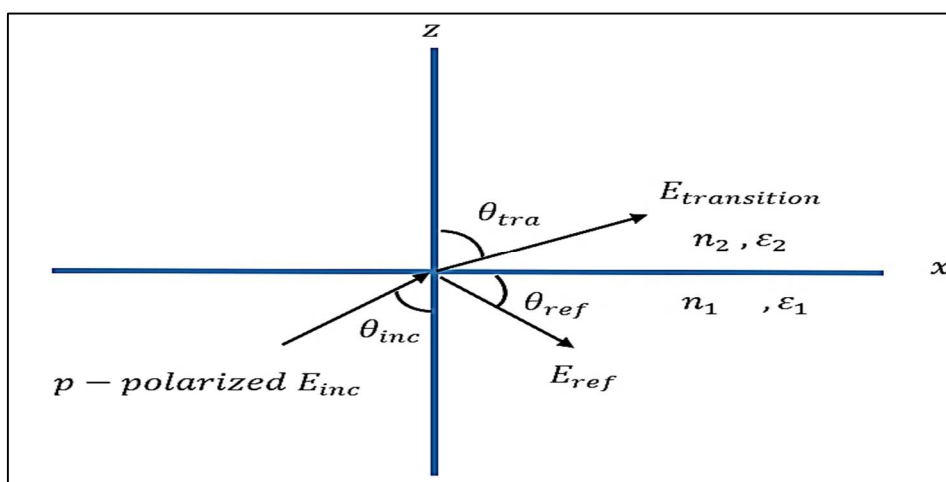


Figure 2: Prism technique for p-polarization in different media in refractive index and dielectric

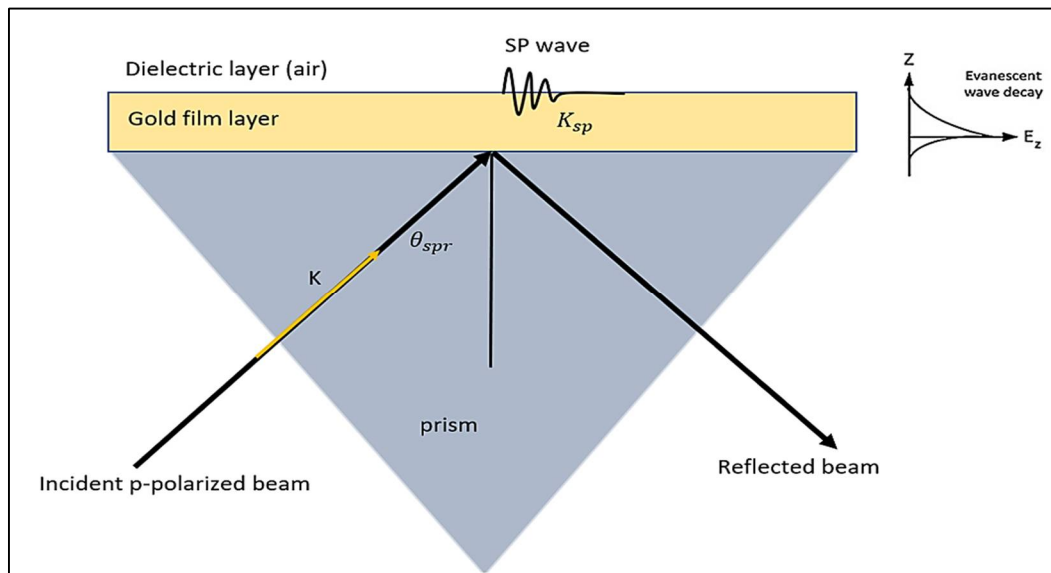


Figure 3: Evanescence wave in gold/air interface

## 2. Materials and Methods

The wavelengths of the laser beam monochromatic source were fixed at  $632.8\text{nm}$ , and a lens with a focal length of  $10\text{cm}$  was employed to focus the light. All metal films in the studies were formed of a range of nanometer gold placed on a prism, and the film's excitation surface interactions with a dielectric medium, air (refractive index is 1). We used the spin coating method to make a thin film and began by creating a layer with a total thickness of  $10\text{ nanometers}$ . Then we used the same technique to coat the other layer on the slide. The thickness of thin films is measured by scanning the sample with an atomic force microscope (AFM) tip. The dimensions of the substrate are not a critical factor in our work, but we typically employed a  $1.5\text{-centimeter}$  square. We focused on the spot interaction between light and layer film. The substrate was constructed of prism-formed glass with an index of refraction of  $1.51$ . Measurement of reflectance as a result of the angle of incidence can also be used to calculate SPR. At a specific angle, a photodetector can also be used to detect the minimum reflection intensity, referred to as the dark area or SPR angle. It means the massive amount of energy of light converted to electrons metal. Hence the minimum light returned to the detector is known as  $R_{min}$ , as shown in diagram (4). This was done to determine the optimal metal layer thickness for generating SPR and the source angle capable of exciting the SPR modes or SPW. The parallel component of the incoming light's  $k$  - vector is equaled to the parallel  $k$  - vector of the surface plasmon once the incident angle of the beam is equivalent to the resonance angle (also named the Attenuated Total Reflection angle ( $\theta_{ATR}$ )). Hence the minimum light returned to the detector (not reflected), as can be seen in Figure 4. The energy of incoming light is converted to oscillations of metal film electrons at that spot, and the accumulating oscillations of metal film electrons are referred to as the evanescence field or SPR [12].

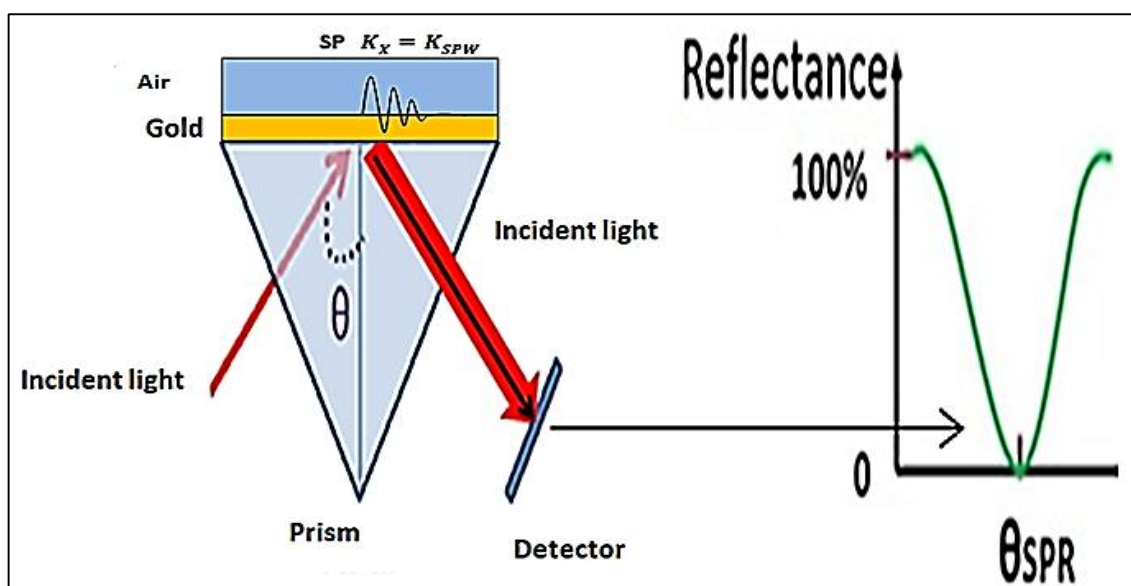


Figure 4: Minimum reflection at  $\theta_{spr}$

SPR occurs at the interface of both the metal sheet and the second medium (dielectric layer). The interaction between them is determined by the surface plasmon wave vector ( $k_{spw}$ ).

$$k_{spw} = k_0 \sqrt{\frac{\epsilon_{material} \epsilon_{dielectric}}{\epsilon_{material} + \epsilon_{dielectric}}} \tag{2}$$

For Equation (2) see [12]. Where  $k_0$  is the optical wave's free space wave vector, which may be expressed as:

$$k_0 = \frac{2\pi}{\lambda_0} \tag{3}$$

$\lambda_0$ : wavelength of the normal projection beam. The terms denote the metal's dielectric and medium's dielectric characteristics.  $\epsilon_{metal}$  and  $\epsilon_{dielectric}$ . The SPW could be strongly tied to the beam's energy. The following is the relationship between  $k_x$  and incident light angle:

$$k_x = k_0 n_{glass} \sin \theta_{in} \tag{4}$$

The angle of incident and index of refractive are indicated by the terms  $n_{glass}$  and  $\theta_{in}$  accordingly. In a glass-metal-dielectric system, excitation of plasmon at the interface among metal and the dielectric surface is governed by the following condition:

$$k_x = k_0 \tag{5}$$

For the equations above, see [13-15] above  $k_x$ : surface plasmon interface wave vector. To create resonance, the wave vector of the incident beam is focused on the interface, aligned with the propagating wave of the surface plasmon oscillations, as seen in Equation (4). A dip absorption in the reflectance can be seen when the incident light meets the resonance threshold [13, 15]. In addition, for varied thicknesses, the incident angle was recorded at the same time. We were using a simpler N-layer model to create an SPR curve and determine the reflectivity of light. The z-axis is used to arrange all the layers.

thickness layer ( $d_k$ ), dielectric constant ( $\epsilon_k$ ), permeability ( $\mu_k$ ). Initially, there were tangential fields  $z = z_1 = 0$  and at the final limit  $z = z_{N-1}$  [15, 16] are provided by

$$\begin{bmatrix} U_1 \\ V_1 \end{bmatrix} = M \begin{bmatrix} U_{N-1} \\ V_{N-1} \end{bmatrix} \tag{6}$$

$U_1, U_{N-1}$  are the electric field components,  $N_{th}$  is layers of the structure, respectively,  $V_1$  and  $V_{N-1}$  are the magnetic field elements, and M is the structure's feature matrix, given by:

$$M = \prod_{K=2}^{N-1} M_K \tag{7}$$

$$M_K = \begin{bmatrix} \cos \beta_k & -i \sin \beta / q_k \\ -i \sin \beta / q_k & \cos \beta_k \end{bmatrix} \tag{8}$$

Where

$$q_k = [\epsilon_k + n_1^2 \sin^2 \theta]^{1/2} \epsilon_k^{-1} \tag{9}$$

And

$$B_k = \left(\frac{2\pi d_k}{\lambda}\right) [\epsilon_k + n_1^2 \sin^2 \theta]^{1/2} \tag{10}$$

$B_k$ : face factor. The amplitude reflection coefficient ( $r_p$ ) for p-polarized light is:

$$r_p = \frac{(M_{11} + M_{12} qN) q_1 - (M_{21} + M_{22} qN) qN}{(M_{11} + M_{12} qN) q_1 + (M_{21} + M_{22} qN) qN} \tag{11}$$

For polarized light, the N-layer model's reflection coefficient is:

$$R_P = |r_p|^2 \tag{12}$$

The equations above are referenced in [15,16]

### 3. Results and Discussion

The parameters for refractive index ( $n_{air} = 1.33$ ,  $n_{gold} = 0.18$  and  $n_{prism} = 1.515$ ). were used to do calculations of SPR for a metal film on a prism in the air for  $632.8nm$  wavelength monochromatic p-polarization. For a given wavelength, the minimal reflectance was recorded at an angle of incidence between  $(45.1^\circ - 46.3^\circ)$ . Comparison of sharp dip curves amongst themselves to establish the best curve at a certain thickness indicates that the optimum SPW occurs at a specific angle. SPR's best curves are depicted in Figure 5. The (SPR) can emerge when light impacts a thin metal layer under total internal reflection (TIR) conditions, which means resonance occurs at a critical angle (SPR angle) of incident light. According to Snell's Law, the total internal reflection happens at a range of  $(40 - 50)^\circ$ . For our research,  $(40)^\circ$ , the data is useless because all incident light is nearly back to the detector nothing is happening (SPR not happen), or no (TIR) happens. The same statement is true for the range of greater  $(50)^\circ$ . That is why we took data in that range [17, 18]. Figure 5 could be obtained from recorded data of the reflection of the laser beam for each layer by varying incident angles. The possible angle for producing SPR is  $(40 - 50)^\circ$ .

As can be observed, even the tiniest amount of reflection would be noticeable at a given angle and thickness. Theoretically, once the thickness of a gold metal sheet goes beyond  $70nm$ , the SPR curve (deformation) vanishes; yet, the same statement is true for thicknesses lower than  $20nm$  that clearly appeared in Figure 5 due to a lack of enough thickness's metal to absorb the energy of light and to create plasmon oscillations, as a consequence, optimum thickness's metal is a critical key for the SPR approach. According to Table 1, a specific angle (resonance angle) might be suitable for producing SPW or evanescent waves. They generated by total reflection were launched at the gold/air contact. When incident light interacts with the surface layer, energy is transmitted to electrons, creating electron excitation inside the metal [19]. Figure 6 shows that the greatest reflectance occurs at a thickness of  $50nm$  of the gold layer at an angle of  $45.4^\circ$ , which is the ideal thickness for generating SPR. The FWHM corresponding to  $\Delta\theta$  is roughly  $0.55^\circ$  at the same layer  $50nm$ , indicating that this region is highly sensitive to shift(change) and so might be employed as a biosensor. In comparison, our result (*thickness* =  $50nm$ ) exhibits dip reflection at  $45.2^\circ$ , which is fairly identical to other results, which are  $44.5^\circ$ , as done in [15].

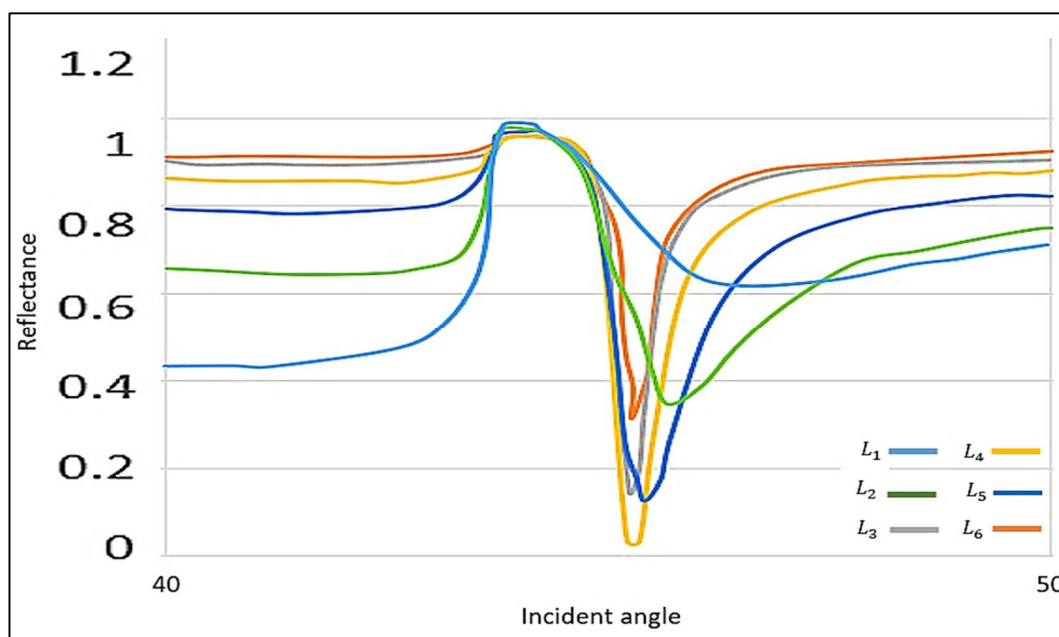


Figure 5: Reflectance as a function of incident angle of gold/air interface light-polarization

SPR is a mechanism in which a free electron in a metal can be stimulated by light at a specific angle. Still, without a gold coating on the substrate, nothing happens (no SPR) since there are no free electrons on the surface, which is why a gold coating on the substrate is required to produce SPR. When examining the effect of film thickness on SPR, the number of layers should be considered when investigating the influence of film thickness on SPR. When the number of layers  $L$  increases, the resonance peak shifts somewhat, the dip sharpness and dip amplitude vary, and the size of the peak changes and changes, becoming larger, respectively. As the number of layers rises, the plasmonic angles vary between  $45.1^\circ$  to  $46.3^\circ$ , below and above this region, there was no pure reflectance because the resonance conditions were not performed, so SPW became damped gradually [19, 20]. To decrease the impact, we optimize the thickness's gold to achieve the best SPW see Table 1.

The thickness of the metal layer has a significant impact on the surface plasmon resonance, according to our findings. The FWHM (full width half maximum) is a critical parameter for describing peak reflection. We investigated all peaks of gold layer lengths and discovered that the region with the greatest FWHM ( $0.48^\circ - 0.55^\circ$ ) for  $(40 - 50)nm$  thickness, this region is more sensitive than other locations that is illustrated in Table 2.

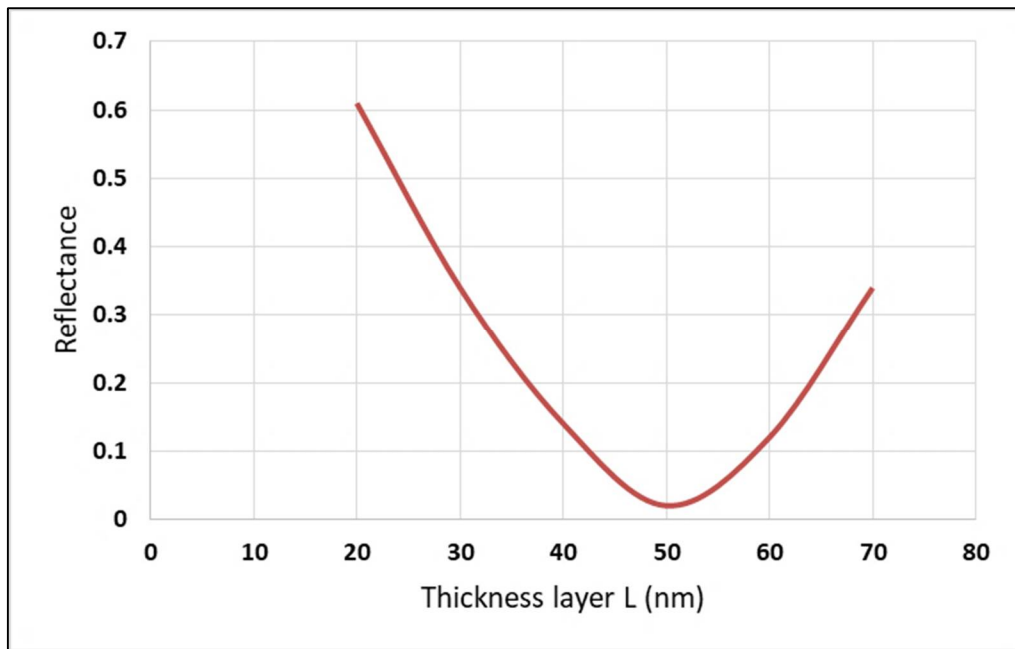


Figure 6: Minimum reflectance for each layer (thickness gold layer)

Table 1: Optimum thickness's metal (gold) concerning the (Number layers) for variations in the resonance angle and minimum Reflectance at 632.8nm

Number layer L	Thickness of gold in nm	Resonance angle recorded $\theta_{spr}$	Minimum reflectance $R_{min}$ in (a.u)
1	20	46.3	0.61
2	30	45.6	0.34
3	40	45.1	0.14
4	50	45.2	0.02
5	60	45.4	0.12
6	70	45.3	0.34

Table 2: FWHM for each layer of gold thickness

L number of layer	Thickness of gold in nm	FWHM corresponding to $\Delta\theta^\circ$
1	20	> 5
2	30	> 5
3	40	0.48
4	50	0.55
5	60	0.72
6	70	0.6

#### 4. Conclusion

SPR is a useful strategy with a wide range of applications in today's world; Therefore, more in-depth investigation is needed to study this. The SPR is done by utilizing the Kretschmann arrangement. The gold/air on the prism could generate the greatest SPR at a certain thickness. In this study, we presented how such a thickness parameter of the gold layer affected the material characteristics of SPRs and observed the crucial angle responsible for generating SPW. We also looked at the effect of the (N-layer) thickness based on the curve's form (sharp dip curve) and the minimum reflectivity peaks, two major criteria that influence the SPR feature. Because the surface plasmons were dissipated, the reflectance does not drop to zero totally. It has been discovered that changing the metal thin layer induces a shift in the resonance angle and resonance dip peak, as well as a change in its amplitude and size. Finally, the SPR might be improved by choosing the optimal metal thickness, resulting in increased sensitivity. In comparison to the theoretical modulation of 43.3°, the best SPR dip was discovered at 45.1° degrees in the region of 40 – 50nm gold film thickness. Biological sensors are one of the many applications for the SPR.

### Author contribution

All authors contributed equally to this work.

### Funding

This research received no external funding

### Data availability statement

The data that support the findings of this study are available on request from the corresponding author.

### Conflicts of interest

Authors declare that their present work has no conflict of interest with other published works.

### References

- [1] K. A. Willets, R. P. Van Duyne, Localized surface plasmon resonance spectroscopy and sensing, *Annu. Rev. Phys. Chem.*, 58 (2007) 267-297. <https://doi.org/10.1146/annurev.physchem.58.032806.104607>
- [2] P. K. Maharana, R. Jha, S. Palei, Sensitivity enhancement by air mediated graphene multilayer based surface plasmon resonance biosensor for near infrared, *Sens. Actuators B Chem.*, 190 (2014) 494-501. <https://doi.org/10.1016/j.snb.2013.08.089>
- [3] H. Nakamura, An enzyme-chromogenic surface plasmon resonance biosensor probe for hydrogen peroxide determination using a modified Trinder, *Biosens. Bioelectron.*, 24 (2008) 455-460. <https://doi.org/10.1016/j.bios.2008.04.022>
- [4] P. K. Maharana, R. Jha, Chalcogenide prism and graphene multilayer based surface plasmon resonance affinity biosensor for high performance, *Sens. Actuators B Chem.*, 169 (2012) 161-166. <https://doi.org/10.1016/j.snb.2012.04.051>
- [5] J. M. Bingham, K. A. Willets, N. C. Shah, D. Q. Andrews, R. P. Van Duyne, Localized Surface Plasmon Resonance Imaging: Simultaneous Single Nanoparticle Spectroscopy and Diffusional Dynamics, *J. Phys. Chem. C.*, 113 (2009) 16839-16842. <https://doi.org/10.1021/jp907377h>
- [6] S. Mohapatra, S. Kumari, R. S. Moirangthem, Fabrication of a cost-effective polymer nanograting as a disposable plasmonic biosensor using nanoimprint lithography, *Mater. Res. Express*, 4 (2017) 076202. <https://dx.doi.org/10.1088/2053-1591/aa764e>
- [7] Y. Chen, Y. Yu, X. Li, Z. Tan, Y. Geng, Experimental comparison of fiber-optic surface plasmon resonance sensors with multi metal layers and single silver or gold layer, *Plasmonics*, 10 (2015) 1801-1808. <https://doi.org/10.1007/s11468-015-9973-7>
- [8] S. K. Srivastava, R. Verma, B. D. Gupta, Theoretical modeling of a self-referenced dual mode SPR sensor utilizing indium tin oxide film, *Opt. Commun.*, 369 (2016) 131-137. <https://doi.org/10.1016/j.optcom.2016.02.035>
- [9] N. H. T. Tran, B. T. Phan, W. J. Yoon, S. Khym, H. Ju, Dielectric Metal-Based Multilayers for Surface Plasmon Resonance with Enhanced Quality Factor of the Plasmonic Waves, *J. Electron. Mater.*, 46 (2017) 3654-3659. <https://doi.org/10.1007/s11664-017-5375-2>
- [10] S. Mohapatra, R. S. Moirangthem, Theoretical study of modulated multi-layer SPR device for improved refractive index sensing, *IOP Conf. Ser. Mater. Sci. Eng.*, 310 (2018) 012017. <https://doi.org/10.1088/1757-899x/310/1/012017>
- [11] R. Kashyap, Enhanced Biosensing Activity of Bimetallic Surface Plasmon Resonance Sensor, *Photonics*, 6 (2019) 108. <https://doi.org/10.3390/photonics6040108>
- [12] P. Zubiarte, C. R. Zamarreño, I. Del Villar, I. R. Matias, F. Arregui, High sensitive refractometers based on lossy mode resonances (LMRs) supported by ITO coated D-shaped optical fibers, *Opt. Express*, 23 (2015) 8045-8050. <https://doi.org/10.1364/oe.23.008045>
- [13] M. F. S. Al-Saady, A. K. H. Albarazanchi, F. S. Mohammed, Design and simulation of localized surface plasmon resonance-based fiber optic chemical sensor, *IOP Conf. Ser.: Mater. Sci. Eng.*, 871 (2020) 012074. <https://doi.org/10.1088/1757-899x/871/1/012074>
- [14] V. R. Sudheer, S. R. S. Kumar, S. Sankararaman, Ultrahigh Sensitivity Surface Plasmon Resonance-Based Fiber-Optic Sensors Using Metal-Graphene Layers with Ti3C2Tx MXene Overlayers, *Plasmonics*, 15 (2019) 457-466. <https://doi.org/10.1007/s11468-019-01035-3>
- [15] W. M. Mukhtar, P. S. Menon, S. Shaari, M. Z. A. Malek, A. M. Abdullah, Angle Shifting in Surface Plasmon Resonance: Experimental and Theoretical Verification, *J. Phys. Conf. Ser.*, 431, 2013, 012028. <https://doi.org/10.1088/1742-6596/431/1/012028>

- [16] Benaziez, S., Z. Dibi, N. Benaziez, Reflectivity optimization of the SPR graphene sensor, *Nanopages*, 13 (2018) 5-17. <https://doi.org/10.1556/566.2018.0023>
- [17] D. Nguyen, Calculating Resonance Angle for Surface Plasmon Resonance Activation on Different Metals. *Undergraduate J. Math. Model.*, 11 (2020) 8. <https://doi.org/10.5038/2326-3652.11.1.4927>
- [18] O. Yeshchenko, I. Bondarchuk, V. Gurin, I. Dmitruk, A. Kotko, Temperature dependence of the surface plasmon resonance in gold nanoparticles, *Surf. Sci.*, 608 (2013) 275-281. <https://doi.org/10.1016/j.susc.2012.10.019>
- [19] Z. Tan, X. Li, Y. Chen, P. Fan, Improving the Sensitivity of Fiber Surface Plasmon Resonance Sensor by Filling Liquid in a Hollow Core Photonic Crystal Fiber, *Plasmonics*, 9 (2013) 167-173. <https://doi.org/10.1007/s11468-013-9609-8>
- [20] N. H. T. Tran, Gold nanoparticles enhanced fluorescence for highly sensitive biosensors based on localized surface plasmon resonance applied in determination C-reactive protein, *Sci. Technol. Dev.J.*, 24 (2021) 867-874. <https://doi.org/10.32508/stdj.v24i1.2489>